

Analyzing protein–protein interactions in cell membranes

Anja Nohe and Nils O. Petersen*

Summary

Interactions among membrane proteins regulate numerous cellular processes, including cell growth, cell differentiation and apoptosis. We need to understand which proteins interact, where they interact and to which extent they interact. This article describes a set of novel approaches to measure, on the surface of living cells, the number of clusters of proteins, the number of proteins per cluster, the number of clusters or membrane domains that contain pairs of interacting proteins and the fraction of one protein species that interacts with another protein within these domains. These data can then be interpreted in terms of the function of the protein–protein interactions. *BioEssays* 26:196–203, 2004.

© 2004 Wiley Periodicals, Inc.

Introduction

The cell membrane is a chemically and physically heterogeneous environment organized through specific lipid and protein interactions into domains of varying composition, size and function. Recent work shows that certain lipids, including cholesterol, sphingomyelin and specific glycolipids, can segregate into small, submicron-sized domains, called rafts.^(1,2) These domains also contain selected proteins, such as the GPI-anchored proteins, and are believed to act as focal points for certain signal transduction events.^(3–10) Caveolae are structures that are similar in composition to the rafts but are characterized by containing a unique family of proteins, caveolins.⁽⁴⁾ There is evidence that some caveolae contain both known isoforms of caveolin-1, caveolin-1 α and caveolin-1 β , while others are greatly enriched in the caveolin-1 β .⁽¹¹⁾ A coated pit is an assembly of membrane proteins, adaptor proteins and clathrin that serves as a vehicle for internalizing membrane receptors (and their associated ligands). This can lead to downregulation of the membrane receptors and desensitization to the corresponding signals.⁽¹²⁾ The fact that these distinct structures exist and that they may have different functions raises a number of questions: What proteins are associated with which domains? How many of any given protein are

there in each domain? How many different proteins are there in each type of domain? How does the organization of receptors into domains affect their function? To answer these questions, we must study the distribution of proteins associated with the domains directly on the cell surface. We need tools to quantify the distribution of proteins and their location in domains.

Fig. 1 illustrates schematically the types of interactions that we need to explore. First, we need to explore the interaction of a protein with itself—this we describe as protein aggregation (Fig. 1A). We are interested in how many aggregates or clusters there are per unit area (the cluster density) and how many protein units there are in each aggregate or cluster (the degree of aggregation). Second, we need to measure the interaction between two different proteins—this we describe as protein association (Fig. 1B,C). We need to examine how many clusters contain both proteins of interest (the density of mixed clusters) and what fraction of each protein interacts with the other (the extent of co-localization or association). Intermolecular interactions occur in at least two ways—association of pairs of membrane proteins, as in Fig. 1B, or association of membrane proteins with soluble proteins in the cytoplasmic or the extracellular environment, as in Fig. 1C.

While we need tools that can measure, at the individual cell level, the cluster density, the degree of aggregation and the extent of association of proteins, we must also recognize the need to sample large numbers of cells. There is mounting evidence that properties associated with individual cells in a population of cells, particularly when studied in cell cultures, vary widely. Multiple measurements on a single cell generally show less variation than single measurements on multiple cells. The population variation often exceeds the precision with which a measurement on a single cell can be made. This suggests that we need to select tools that can easily sample many cells (of the order of hundreds) in a population and can reduce the information to population averages that can be compared under different conditions—with and without stimulation by an agent, as a function of temperature, with and without drugs etc. Finally, we seek methods that are readily applicable to living cell cultures or tissues and can explore the dynamics as well.

In this article, we describe a pair of tools designed to provide quantitative measures of the desired parameters (cluster density, degree of aggregation, extent of co-localization) on large numbers of cells. The tools require that we collect high-resolution fluorescence images of specific proteins

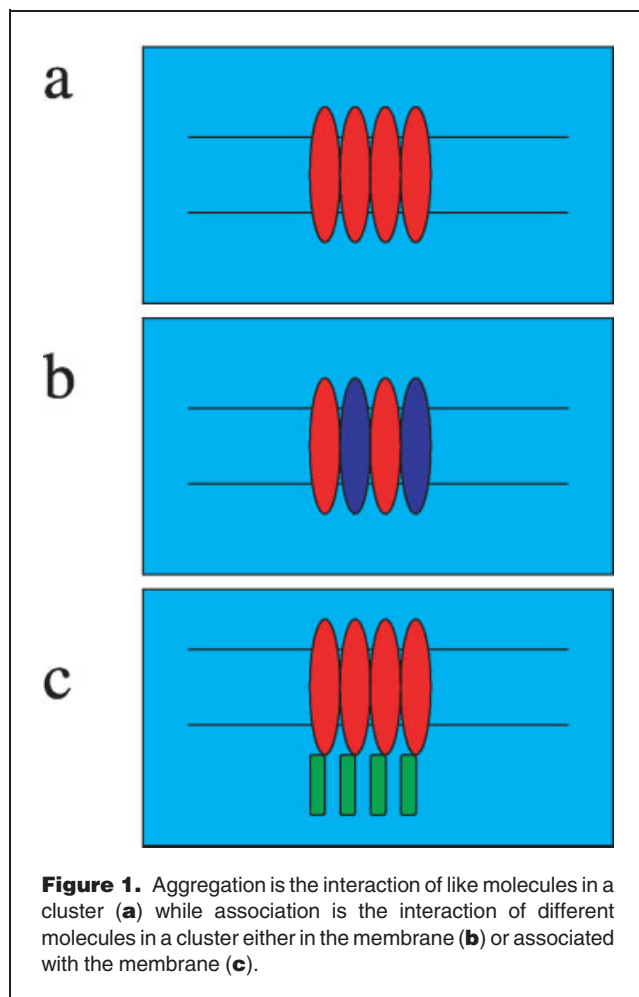
Department of Chemistry, The University of Western Ontario, London, ON N6A 5B7, Canada

*Correspondence to: Nils O. Petersen, Department of Chemistry, The University of Western Ontario, London ON N6A 5B7, Canada

E-mail: petersen@uwo.ca

DOI 10.1002/bies.10380

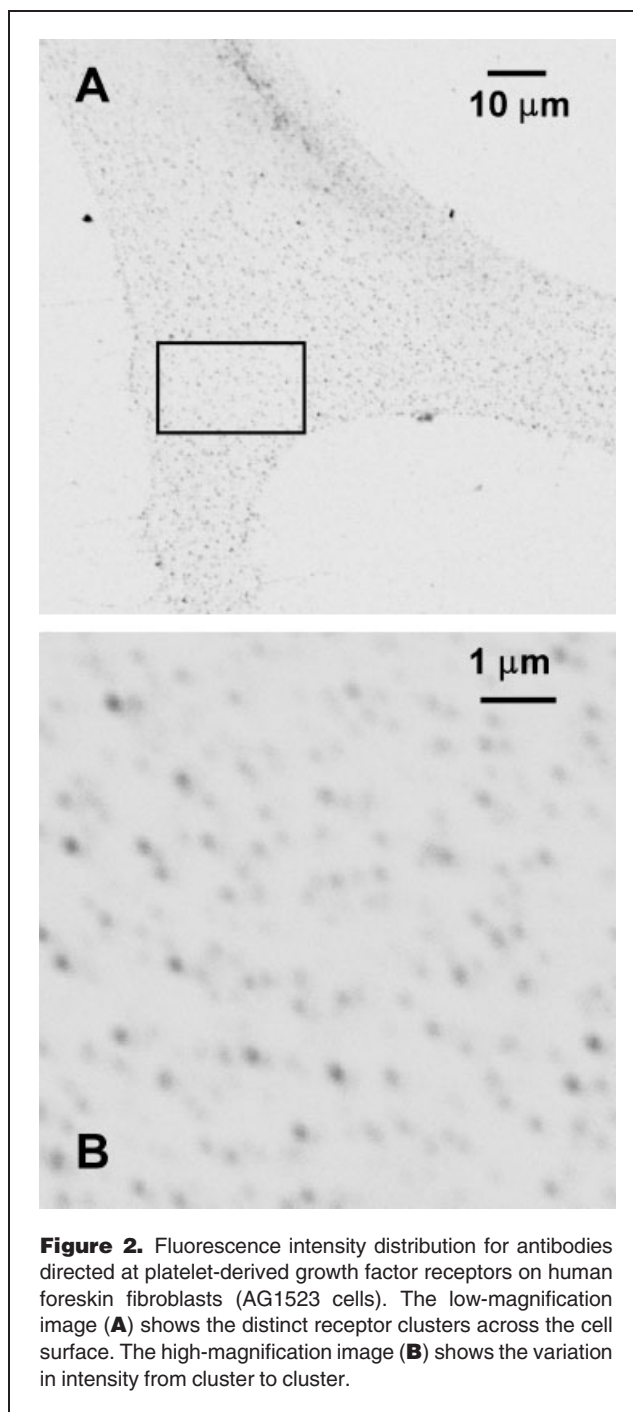
Published online in Wiley InterScience (www.interscience.wiley.com).



distributions on cell surfaces. Subsequently, we calculate the correlation functions of these images, which provide numerical estimates of the density of molecules or clusters in the images that can be interpreted in terms of the aggregation state and the extent of intermolecular interaction. The tools, called Image Correlation Spectroscopy and Image Cross Correlation Spectroscopy, are rooted in rigorous statistical mechanical principles and based on fundamental mathematical theorems. The quantitative information is therefore based on solid foundations. Interpretation of the information in biological terms may require additional information from biochemical or molecular biological experiments.

Counting aggregates

Fig. 2 illustrates the challenges of measuring protein aggregation. Fig. 2A shows the laser scanning confocal microscopy image of an AG1523 human foreskin fibroblast cell exposed to a fluorescently labeled rabbit antibody that recognizes the Fc-portion of a monoclonal mouse antibody directed exclusively at the β -isoform of the platelet-derived growth factor receptor



(PDGF-R- β).⁽¹³⁾ Fig. 2B shows the confocal image of a section of the cell membrane of the same cell collected at 10-fold higher magnification. Each PDGF-Receptor should be represented by a particular fluorescence intensity and therefore the intensity at specific pixels in the image measures both where the receptor is located and the number of receptors at each location. In the absence of background noise, it is, in

principle, possible to determine the location of each cluster of molecules in the image and the number of molecules in each cluster at each location. One can determine where the maxima of the intensity are and calculate the integrated intensity in each region. In reality, this analysis is less than trivial. First, one must determine which maxima represent real clusters and which derive from noise. Second, one must count the number of clusters in the image and determine the intensity of each, which can be done using appropriate fitting routines. Third, one must determine the fluorescence intensity per molecule, a number that depends on excitation efficiency and emission detection effectiveness. This has been attempted,⁽¹⁴⁾ and a detailed analysis yields the distribution of the number of molecules per cluster as well as the average number of molecules per cluster and the total number of clusters. However, in practice, when the noise in the signal is significant, the analysis of each individual cluster is not reliable.

The image correlation spectroscopy approach averages all of the information from all of the clusters in an image into a single number representing the average number of clusters. The detailed spatial information is lost but the analysis provides an accurate estimate of the average number of clusters per unit area in addition to the average intensity per pixel. This allows for analysis and comparison of many images collected on different cells to yield useful population average data. In the next section, we explain the principles of data collection, analysis and interpretation and evaluate the merits of these approaches relative to others.

Fluctuation amplitudes depend on average numbers

Fig. 2B shows distinct fluorescence located in spatially resolved clusters. It also shows that there are different intensities associated with each of these clusters, but each cluster has the same physical dimension—here determined by the size of the laser beam in the confocal microscope. Thus each cluster represents a collection of molecules contained in a region smaller than the dimension of the focused laser beam—of the order of 300 nm in radius. Our objective is to get a reliable measure of the number of clusters per unit area and the average number of receptors per cluster. To achieve this objective, *we rely on a well-known statistical mechanical principle that equates the variance of the relative fluctuations in concentration in a small volume with the inverse of the average number of molecules in that volume.*⁽¹⁵⁾ For example, if there are many molecules in a small volume, the relative concentration fluctuations will be small, whereas if there are only a few molecules in the volume, the relative concentration fluctuations will be large¹.

¹The standard deviation of the fluctuations scales as the square root of the number of molecules in the volume so the standard deviation of the relative fluctuation scales as the inverse of the square root of the number of molecules in the volume.

This relationship between fluctuation amplitude and average number is exploited in concentration or fluorescence correlation spectroscopy measurements. Fluorescence Correlation Spectroscopy (FCS) measures temporal variations in fluorescence intensity emanating from the small volume at the focal point of a stationary laser beam.⁽¹⁶⁾ The amplitude, $g(0)$, of the normalized autocorrelation function, $g(\tau)$, is calculated as an estimate of the variance of the relative intensity fluctuations, which in turn yields an estimate of the average number of fluorescent particles in the focal volume. FCS analysis requires observation of many characteristic fluctuations, which for cell surface proteins takes such a long time that it has been impractical to implement reliably.

Image Correlation Spectroscopy (ICS) measures spatial variations in fluorescence intensity emanating from the large number of small volumes detected in the image as the laser beam scans through the sample. The amplitude, $g(0,0)$, of the normalized autocorrelation function, $g(\xi,\eta)$, provides the corresponding estimate of the average number of fluorescent particles in each of the focal volumes. In this case, the dynamics is imposed by the experiment and the inherent dynamics of the proteins are lost in a particular image. We argue, however, that the number count obtained from the spatial fluorescence fluctuations in an ICS experiment is the same as that which could be obtained from the temporal fluorescence fluctuations in the FCS experiment. Since the focus is on understanding the state of aggregation, losing other information is acceptable.

Both FCS and ICS applications use the autocorrelation function as a tool to estimate the number counts. This is, in part, because the white noise present in each time channel or image pixel contributes excessively to the variance when it is calculated directly. The only meaningful estimate comes from an extrapolation of the autocorrelation functions. FCS relies on direct calculation of the autocorrelation function, but this is computationally demanding for even moderately sized images. Instead, we use the fact that the autocorrelation function is the Fourier Transform of the Power Spectrum of the image. The Power Spectrum is, in turn, the product of the real and the imaginary components of the Fourier Transform of the original image.

The ICS experiment then consists of obtaining high-quality, high-resolution confocal images of a large number of cells; calculating first the two-dimensional Fourier Transforms of the images, then the power spectra and finally the reverse two-dimensional Fourier Transforms. The resulting autocorrelation functions are fit to a two-dimensional Gaussian function—reflecting the transverse intensity distribution of the laser beam at the cell surface. The amplitude of the autocorrelation function gives the desired estimate of the number of molecules in the area illuminated by the laser beam.

One of the key advantages of the ICS approach is that it uses images generated by confocal microscopy—a tool

commonly available to cell biologists. Generating the raw data on diverse cell populations subjected to desired treatments is, therefore, nearly routine. The mathematical treatment is straightforward and appropriate data analysis programs are available.² There are naturally details in the interpretation that must be understood, but these have been discussed elsewhere.⁽¹⁷⁾

Measuring the degree of aggregation

The total fluorescence intensity in a confocal image must reflect the total number of molecules that are fluorescent. The relationship can be quantified as long as the extinction coefficient and the quantum yield of the fluorophore is known and the collection efficiency function of the microscope and the efficiency of the detector is known. Alternatively, the instrument can be calibrated so that the number of photons detected per molecule at particular illumination intensities can be determined.

Since the image intensity is a measure of the total number of monomers present in the clusters in the image and since the amplitude of the autocorrelation function is an estimate of the inverse of the average number of clusters in the image, the product of the intensity and the amplitude of the autocorrelation functions provides a measure of the degree of aggregation—that is the average number of monomers per cluster.

As an example to illustrate the point, this analysis was performed in detail for the receptor system shown in Fig. 2. In this case, the data for hundreds of measurements on hundreds of cells, show that on average there are seven clusters per square micrometer (the cluster density) and that there are 3.3 molecules per cluster (the degree of aggregation). We measure the average surface area of these cells to be about $10,000 \mu\text{m}^2$, indicating that there must on the order of 200,000 receptors per cell.⁽¹⁸⁾ This compares favorably to the estimate of about 150,000 receptors per cell measured by standard biochemical binding assays. Thus, ICS analysis will provide estimates of the cluster density and the degree of aggregation that are accurate to within about 25%.

Identifying protein associations and quantifying co-localization

Fig. 3 shows two high-resolution confocal microscope images measured sequentially on the same region of the same cell. Fig. 3A depicts the fluorescence of antibodies directed at clathrin—the major structural protein in coated pits.⁽¹²⁾ Figure 3B depicts the fluorescence of antibodies directed at a membrane protein engineered to interact with the adaptor

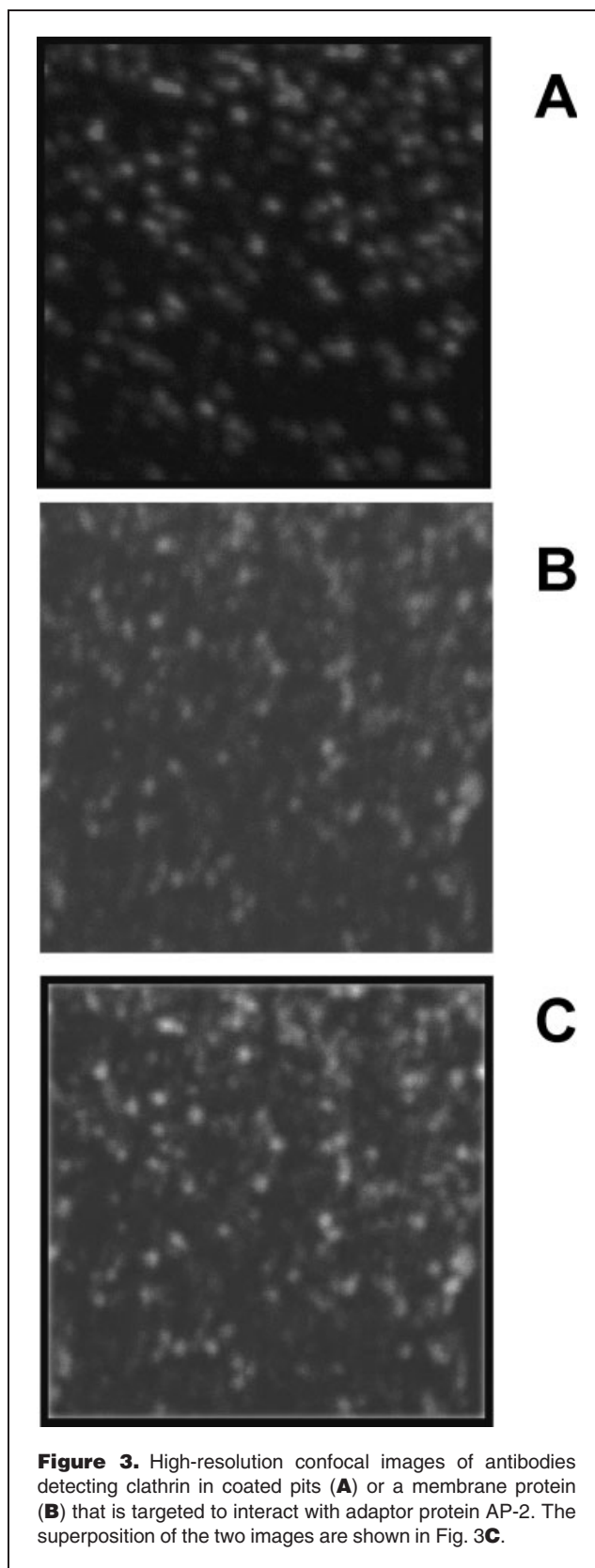


Figure 3. High-resolution confocal images of antibodies detecting clathrin in coated pits (**A**) or a membrane protein (**B**) that is targeted to interact with adaptor protein AP-2. The superposition of the two images are shown in Fig. 3**C**.

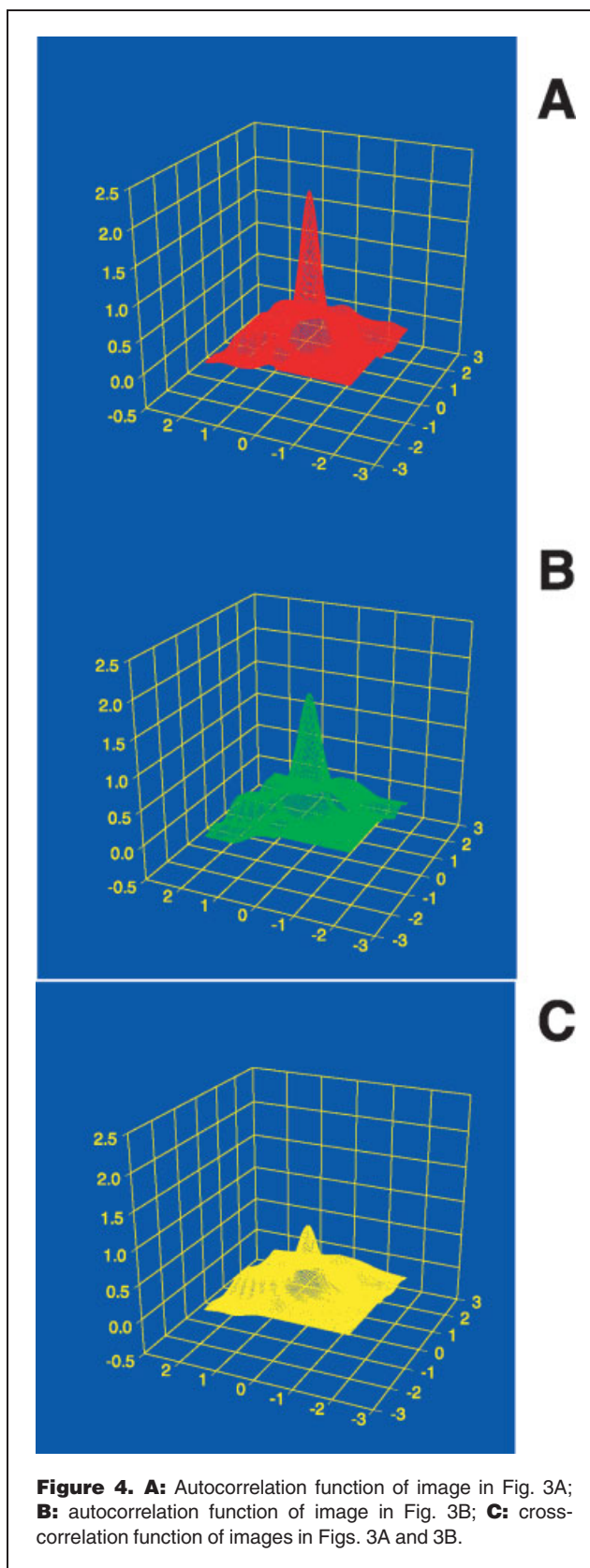
²Paul Wiseman, Department of Chemistry, McGill University or Nils Petersen, Department of Chemistry, The University of Western Ontario can be contacted for further information.

protein in coated pits^{3,(19)} Since coated pits play a crucial role in endocytosis, it is important to understand the distribution of proteins in these domains. The specific questions of interest are: what is the proportion of membrane protein in coated pits relative to that not in coated pits and what proportion of the coated pits contain this particular membrane protein—none, some or all? The classical approach to investigating these questions is to overlay the images as shown in Fig. 3C. Because of the colour schemes used in the images, those regions in the image where the membrane proteins are located in the coated pits will be yellow. In reality, there is a range of colours—orange to yellow—depending on the relative proportion of the red and the green intensities in the original images. It is possible to analyze the details of the co-localization by counting the number of regions representing the pure membrane protein (green), the pure coated pits (red) and the mixed membrane protein-coated pit complexes (orange-yellow). In addition to being tedious, this process is also highly subjective.

Noting that co-localization requires that the intensities in the red and green images are spatially coincident, it is evident that there must be a corresponding coincidence in the intensity fluctuations in the two images: the intensities in the two colours must be spatially correlated. The extent to which the intensity fluctuations are correlated, will be a measure of the extent to which the proteins are co-localized. Image Cross-Correlation Spectroscopy is the tool that we use to estimate the extent of co-localization. It involves calculating the autocorrelation functions of each of the two images to estimate the average cluster density of the membrane proteins and the coated pits separately and then calculating the cross-correlation function between the two images to estimate the average density of clusters that contain both proteins. Comparison of these values provides a quantitative estimate of the fraction of the membrane protein clusters that are associated with coated pits and the fraction of coated pits that contain the membrane proteins.

Fig. 4 shows the autocorrelation functions calculated from the two images shown in Fig. 3 as well as the cross-correlation function calculated between these two images. As discussed above, the amplitude of the autocorrelation function is *inversely* proportional to the average number of clusters and it is evident in this specific example that the average number of clusters in the two images are comparable. The cross-correlation function, however, is *directly* proportional to the average number of clusters with both proteins present.^(19,20) Thus, if there is no co-localization, the cross-correlation

³The membrane protein is a variant of the hemagglutination (HA) protein from influenza virus with a sequence of eight amino acids (YDYKSEYN) added to the cytoplasmic tail and designed such that the YKSF sequence targets it for interaction with AP-2 in the coated pits. This membrane protein was created by Michael Roth (US) and was used in collaborations with Yoav Henis (Israel) by Claire Brown in her thesis work.



function is zero, while if there is complete co-localization the cross-correlation function is maximal. As reported previously, it is relatively easy to measure these images and calculating the corresponding correlation functions for a large number (hundreds) of individual cells to get good estimates of the extent of co-localization. For this membrane protein and using either clathrin or the adaptor protein as the marker for coated pits, it was shown that, on average, 25% of the membrane protein resides inside the coated pits and 75% is outside the coated pits. On the other hand, all of the coated pits contain the membrane protein.

It should be noted that, in this analysis, the cross-correlation function reflects co-localization within the limit of resolution dictated by the optics, on the order of 300 nm. There is no requirement for physical contact or direct association of the two proteins being measured, but there must be a mechanism that causes them to distribute within the same small region on the surface. This could be partitioning into rafts or caveolae because of the distinct membrane composition or binding to common proteins in structures such as caveolae or coated pits. This spatial resolution limitation distinguishes the image cross-correlation spectroscopy measurement from the temporal fluorescence cross-correlation spectroscopy measurement. In the latter case, the temporal coincidence of fluctuations in the two channels can only arise if the two partners move together into and out of the observation volume. They must therefore be physically associated with each other. The ICCS measurement is less informative than the corresponding FCS measurement, but it can still provide valuable insights into the general association patterns of proteins on the cell surface.

Observing changes in protein distributions

Given that the cell surface is a dynamic environment where diffusion is reasonably facile, one may expect that the protein distribution will change with time, particularly if the cells are stimulated or exposed to a change in their environment. In recent experiments, the distribution of the bone morphogenetic protein receptor type Ia (BRIa) was measured on the surface on normal A431 cells and on the surface of A431 cells grown without serum for 72 hours (starved cells). The average intensity of fluorescence is the same on the two sets of cells indicating that the average receptor concentration remains the same—there is neither upregulation nor downregulation of the BRIa receptor. The average cluster density (CD), measured by ICS, increases by about a factor of two in the starved cells, suggesting that there are twice as many BRIa-containing clusters on the surface. Correspondingly, the degree of aggregation (DA) is decreasing by about a factor of two in the starved cells, suggesting that the average number of BRIa monomers per cluster is halved. The effect of removing the serum from the growth medium for these cells is therefore a dispersal of the BRIa receptors into more, but smaller clusters. As reported elsewhere,⁽²¹⁾ this change in the cluster density may be physiologically important since starvation leads to a corresponding appearance of the bone morphogenetic protein receptor type II (BRII) on the surface of the A431 cells. Since it is known that these two receptors must interact for signaling to occur,^(22,23) it is possible that the redistribution of the BRIa into more but smaller clusters is a driven by the need to interact with the BRII receptor as it emerges on the surface as in Fig. 5.

Receptor distributions are likely to change on a faster time scale than in the BRIa example. To follow these will simply

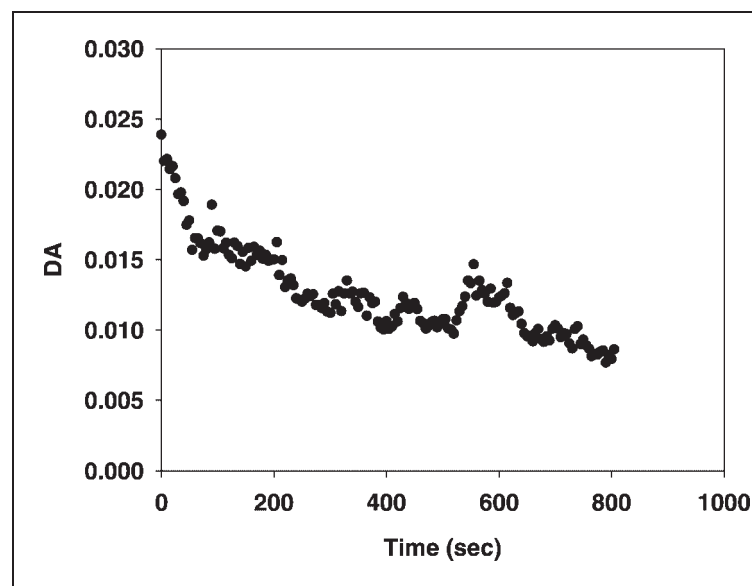
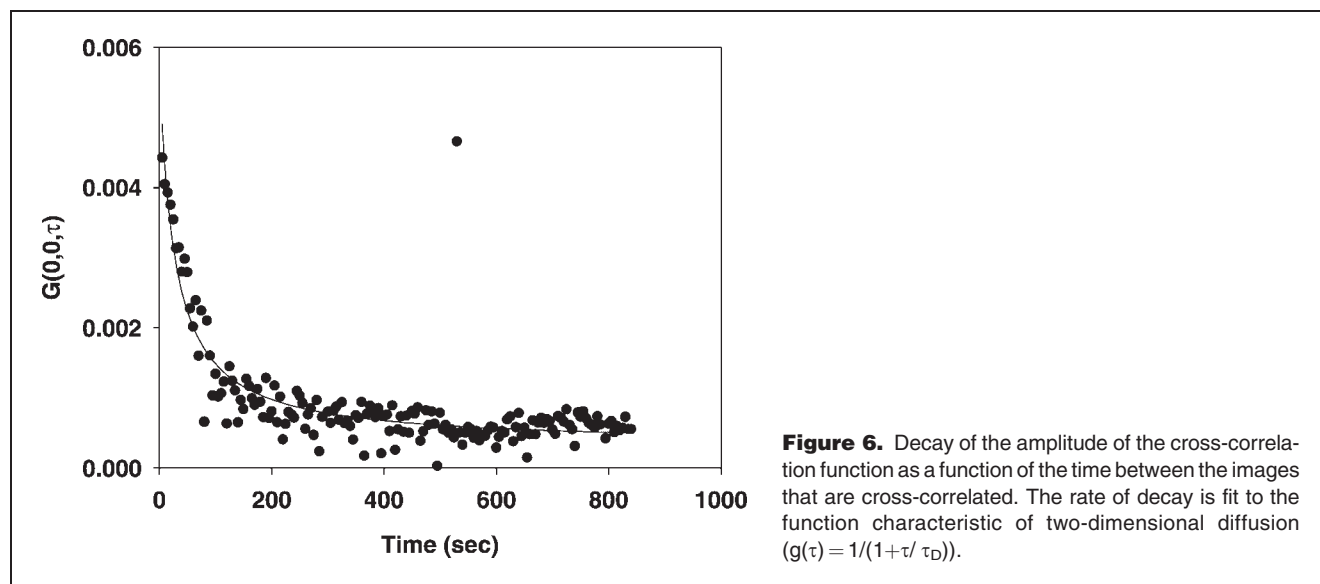


Figure 5. Temporal variation in the degree of aggregation (DA) of a GPI-anchored protein on the surface of cos cells.



require collecting images as a function of time from the same area of a cell. The variation in intensity, cluster density and degree of aggregation can then be monitored directly in the live cell. Fig. 6 provides an example of this for a GPI-anchored protein⁴ transfected into cos cells. Images were collected at 37°C at 10 second intervals and each image was subjected to ICS analysis. The degree of aggregation was calculated as the product of the average intensity and the amplitude of the autocorrelation function for each image. There is a general decrease in the DA as a function of time because of a small, but significant, bleaching of the region of the cell as each subsequent image is collected from the same area. Superimposed on this steady decrease there are small fluctuations in the degree of aggregation, which can be interpreted as small variations in the average number of monomers in each of the clusters of the protein on the surface. In this case, this would suggest that the number of GPI-anchored proteins in the rafts is continually varying around some average value. The variations can be as much as 30% and occur on the time scale of seconds to minutes, which suggests that the sizes of rafts are fluctuating fairly rapidly, perhaps as molecules are moving in and out of the domains.

Since the images used to generate the data in Fig. 6 are collected from the same region of the same cell over a period of time, the images are detecting the same domains from image to image. If the domains were static, the cluster distribution from image to image would remain the same and hence the spatial fluctuations in intensity from one image to the next would be identical. Thus, a cross-correlation function between

temporally adjacent images would show complete coincidence in the intensity fluctuations—there would in effect be complete co-localization from image to image. However, if the domains move, then the cross-correlation function would decrease. It is possible to show that the decay in the cross-correlation function as a function of delay time between images will look like the decay of a temporal autocorrelation function in an FCS experiment.⁽²⁰⁾ Fig. 6 shows the amplitude of the cross-correlation function as a function of the difference in time between pairs of images. The function decays to zero indicating that all the clusters are mobile on this time scale. Moreover, the rate of decay can be fit well to the expected rate of decay for a two-dimensional diffusion problem⁵ ($g(\tau) = 1/(1 + \tau/\tau_D)$). In this particular case, the rate of decay is consistent with a diffusion coefficient on the order of $2 \times 10^{-11} \text{ cm}^2 \text{ s}^{-1}$, which is at least three orders of magnitude slower than the diffusion coefficient of free molecules in the membrane.⁽²⁴⁾ This suggests that the dynamics is that of the cluster (or rafts) rather than the dynamics of the individual GPI-anchored proteins. It is interesting to note that the characteristic time for decay of the cross-correlation function is on the same time scale as the fluctuations in the degree of aggregation seen in Fig. 6. It is therefore likely that the dynamic process that leads to changes in the size of the rafts is also leading to movement across the surface.

Application of ICS or ICCS to images collected as a function of time brings these techniques back to the realm of regular FCS. In fact, the data in Fig. 6 can be thought of as an ensemble-averaged FCS experiment, in which the FCS

⁴This GPI-anchored protein was labeled with green fluorescent protein and expressed in cos cells. This is part of an ongoing collaboration with Gisou van der Goot (University of Geneva).

⁵It should be noted that the decay can also be fit well to an exponential decay, which would be indicative of a dynamic process in which the domains appear or disappear from the surface at a characteristic average rate.

experiment is conducted simultaneously at all points in the image. The time scale for this 'FCS' experiment is limited by the rate of image acquisition, which is now approaching milliseconds or better. Thus the dynamic image correlation spectroscopy approach is bridging a time domain inaccessible to normal FCS experiments.

Bringing it all together

Proteins distribute on the surface of living cells into regions and domains containing more than one species and multiple copies of any given species. The heterogeneous distribution may be related to function, since proximity of the same and different species may enhance intermolecular interactions, leading to more rapid responses to external stimuli. The family of image correlation spectroscopy tools (Image Correlation Spectroscopy, Image Cross-Correlation Spectroscopy and Dynamic Image Correlation Spectroscopy) provides for the first time a consistent approach to measure quantitatively the distribution of protein, the interactions among proteins and the dynamics of the resulting clusters or domains of proteins. The key advantages of these tools are that they can be applied to living cells, that they allow for easy measurements on large numbers of cells and that they employ fairly commonly used confocal microscopy measurements as the starting point. While the measurements are relatively easy, they require some care. The image analysis is straightforward, using standard two-dimensional image analysis tools such as Fourier Transforms. The most-difficult aspect is the actual interpretation of the information. As with many other biophysical tools, they only make sense in the context of the biology. It is therefore important that the experimental protocols deal with the appropriate biological variables and that all the necessary control experiments are also performed. With these caveats, however, image correlation spectroscopy has the potential to provide extensive insights and key information on the intermolecular interactions that are needed at the cell membrane to regulate cell–cell communication.

References

1. Simons K, Ikonen E. Functional rafts in cell membranes. *Nature* 1997;387:569–572.
2. Brown DA, London E. Functions of lipid rafts in biological membranes. *Annu Rev Cell Dev Biol* 1998;14:111–136.
3. Janes PW, Ley SC, Magee AI, Kabouridis PS. The role of lipid rafts in T cell antigen receptor (TCR) signalling. *Semin Immunol* 2000;12:23–34.
4. Schlegel A, Pestell RG, Lisanti MP. Caveolins in cholesterol trafficking and signal transduction: implications for human disease. *Front Biosci* 2000;5:D929–932.
5. Kasahara K, Watanabe K, Takeuchi K, Kaneko H, Oohira A, Yamamoto T, Sanai Y. Involvement of gangliosides in GPI-anchored neuronal cell adhesion molecule TAG-1 signaling in lipid rafts. *J Biol Chem* 2000;275:34701–34709.
6. Fielding CJ, Fielding PE. Cellular cholesterol efflux. *J Lipid Res* 1997;38:1503–1521.
7. Ikonen E, Parton RG. Caveolins and cellular cholesterol balance. *Traffic* 2000;1:212–217.
8. Huang CS, Zhou J, Feng AK, Lynch CC, Klumperman J, DeArmond SJ, Mobley WC. NGF signaling in caveolae-like domains at the plasma membrane. *J Biol Chem* 1999;274:36707–36714.
9. Zhang W, Tribble RP, Samelson LE. LAT palmitoylation: its essential role in membrane microdomain targeting and tyrosine phosphorylation during T cell activation. *Immunity* 1998;9:239–246.
10. Kawabuchi M, Satomi Y, Takao T, Shimonishi Y, Nada S, Nagai K, Tarakhovsky A, Okada M. Transmembrane phosphoprotein Cbp regulates the activities of Src-family tyrosine kinases. *Nature* 2000;404:999–1003.
11. Fujimoto T, Kogo H, Nomura R, Ume T. Isoforms of caveolin-1 and caveolar structure. *J Cell Sci* 2000;113:3509–3517.
12. Bonifacino JS, Traub LM. Signals for Sorting of Transmembrane Proteins to Endosomes and Lysosomes. *Annu Rev Biochem* 2003;72:395–447.
13. Petersen NO, Brown C, Kaminski A, Rocheleau J, Srivastava M, Wiseman PW. Analysis of membrane protein cluster densities and sizes *in situ* by image correlation spectroscopy. *Faraday Discussions* 1998;111:289–305.
14. Morrison IEG, Anderson CM, Georgiou GN, Stevenson GVV, Cherry RJ. Analysis of receptor clustering on cell surfaces by imaging fluorescent particles. *Biophys J* 1994;67:1280–1290.
15. Davidson N. *Statistical Mechanics*. New York: McGraw-Hill; 1962.
16. Elson EL, Webb WW. Concentration Correlation Spectroscopy-New Biophysical Probe Based On Occupation Number Fluctuations. *Annual Review of Biophysics and Bioengineering* 1975;4:311–334.
17. Petersen NO, Riegler Elser, Springer Verlag, editors. *Spatial Correlation Spectroscopy*, Chapter 8 in *Fluorescence Correlation Spectroscopy*, 2001.
18. Wiseman PW, Petersen NO. Image correlation spectroscopy. II. *Biophys J* 1999;76:963–977.
19. Brown CM, Petersen NO. An image correlation analysis of the distribution of clathrin associated adaptor protein (AP-2) at the plasma membrane. *J Cell Sci* 1998;111:271–281.
20. Srivastava M, Petersen NO. Diffusion of transferrin receptor clusters. *Biophys Chem* 1998;75:201–211.
21. Nohe A, Keating E, Underhill TM, Knaus P, Petersen NO. Effect of the distribution and clustering of the type I A BMP receptor (ALK3) with the type II BMP receptor on the activation of signalling pathways. *J Cell Sci* 2003;116:3277–3284.
22. Yamashita H, Ten Dijke P, Franzen P, Miyazono K, Heldin CH. Formation of hetero-oligomeric complexes of type I and type II receptors for transforming growth factor-beta. *J Biol Chem* 1994;269:20172–20178.
23. Ten Dijke P, Miyazono K, Heldin CH. Signaling via hetero-oligomeric complexes of type I and type II serine/threonine kinase receptors. *Curr Opin Cell Biol* 1996;8:139–145.
24. Pralle A, Keller P, Florin EL, Simons K, Horber JK. Sphingolipid-cholesterol rafts diffuse as small entities in the plasma membrane of mammalian cells. *J Cell Biol* 2000;148:997.